

AMPLITUDE VARIATION WITH OFFSET (AVO) AND SEISMIC INVERSION FOR KAFR EL-SHEIKH FORMATION [PLIOCENE AGE] IN THE WESTERN PART OF SOUTH BATRA FIELD, NILE DELTA, EGYPT

M.M. GOBASHY⁽¹⁾, S.M. SHARAFELDIN⁽²⁾, A.H. ZAKARIA⁽³⁾ and A.M.S. IBRAHIM⁽⁴⁾

(1) Professor of Geophysics, Faculty of Science, Cairo University.

(2) Professor of Geophysics, Faculty of Science, Cairo University.

(3) Geophysics Consultant.

(4) Geophysicist at Qantara Petroleum Company.

تطبيق مبدأ تغير سعة الموجة السيزمية مع المسافة و الإنعكاس السيزمي للتكوين الجيولوجي كفر الشيخ

(عصر البليوسين) في الجزء الغربي من حقل جنوب بطره، دلتا النيل، مصر

الخلاصة: يهدف هذا البحث إلى توضيح وتأكيد أهمية الطرق السيزمية الحديثة وذلك لتأكيد وتحديد أماكن تجمع المواد الهيدروكربونية بالتكوين الجيولوجي كفر الشيخ (عصر البليوسين) في الجزء الغربي من حقل جنوب بطره بمنطقة دلتا النيل-مصر. يتم استخدام التفسيرات السيزمية ثلاثية الأبعاد وذلك لتحديد التراكيب الجيولوجية الأساسية و التراكيب الجيولوجية الدقيقة التي تؤثر على المنطقة. ويتم عمل هذه التفسيرات عن طريق عمل تجانس بين بيانات الآبار وبين الخطوط السيزمية وينتج من ذلك الخرائط التركيبية الزمنية حيث يتم بعد ذلك تحويلها الى خرائط تركيبية عميقة باستخدام السرعات المقاسة من الآبار. ودراسة تغيير سعة الموجه السيزمية مع المسافة (AVO) وجد أن حقل جنوب بطره يتبع نوع من الفصيلة الثالثة والتي تشير إلى زيادة سعة الموجة السيزمية مع بعد المسافة من مصدر إنبعاث الموجة وتعتبر هذه الطريقة طريقة مؤكدة لإحتمالية وجود الهيدروكربون في المنطقة وليس أداة إستكشافية يعتمد عليها مباشرة بدون عمل التفسير السيزمي. كما تم استخدام الانعكاس السيزمي (Seismic Inversion) وذلك لتأكيد وتحديد أماكن تجمع المواد الهيدروكربونية وأيضاً لمعرفة حدود القنوات والخزانات الخاصة بالمواد الهيدروكربونية.

ABSTRACT: The aim of this research is determining how to use the modern seismic techniques for tracing and determining the hydrocarbon accumulation in Kafr El-Sheikh Formation (Pliocene age) in the western part of South Batra field, Nile Delta –Egypt, by making 3D seismic interpretation to understand the structure setting and to configure the minor structural elements. This interpretation is made by tying the logs with the seismic data. The output is time structural map, by using the wells to eliminate the velocity model the depth conversion had been done.

From the AVO (Amplitude Variation with Offset) analysis and by using the wells data, it is clear that South Batra field is a class III AVO (Increase of negative amplitude with offset).

By using the post-stack seismic inversion to delineate the hydrocarbon reservoir, it facilitates the interpretation of meaningful geological and petrophysical boundaries in the subsurface. The inversion is an inverting the relative acoustic impedance values from the seismic to an absolute acoustic impedance values.

1. INTRODUCTION

The Nile Delta can be considered the earliest known delta in the world. It was described by Herodotus in the 5th Century BC (Said, 1981). The Nile Delta (Ta-Mehet) in Hieroglyphic language means the land of the estuary water. It is one of the oldest intensely cultivated areas on the earth. The Nile Delta is illustrated to be an arcuate delta (arcshaped), as it resembles a triangle or lotus flower when seen from above.

The present Nile Delta covers an onshore area of about 30,000 km² and about an equal size offshore to the 200 m isobath. The southern apex of the delta is located approximately 30 km north of Cairo where the Nile River splits into the western Rosetta branch and the eastern Damietta branch. The delta reaches some 240 km along the Mediterranean coastline and extends to a maximum of 160 km from north to south. Without the Nile Valley and Delta, Egypt is mainly a desert country.

Renewed deltaic deposition began at approximately 3.8MA. The steep structural hinge line and faulted continental shelf created a large amount of

accommodation space with relatively minor progradation of depositional systems. As a result, the primary play consists of slope-channel fairways in all levels. The Plio-Pleistocene systems are the shallowest targets in the basin, which hold the minority of proven reserves.

The Nile Delta basin is the most prolific, prospective gas and condensate province in Egypt. The Nile Delta is the main gas producing province in the northern part of Egypt with approximately 62 TCF proven reserve (Niazi and Dahi, 2010). This could be attributed to the fact that such province started to disclose part of its hidden hydrocarbon reserves as a direct result of using state of the art exploration techniques, in addition to the expanding use of different types of geological and geophysical modeling.

The Plio-Pleistocene systems are the shallowest targets in the basin, which hold a little part of proven reserves.

The proven reservoirs vary in age from Oligocene/Early Miocene to Pleistocene. Proven source rocks include Jurassic coals and shales and the Lower Miocene condensed Qantara Formation shale. Additional source rocks may be present in condensed intervals of Cretaceous, Oligocene and Eocene ages. Following the Tethyan rifting and the opening of Mediterranean in the Jurassic, prominent Cretaceous mixed clastic and carbonate shelf edges aggraded vertically along a steep fault-bounded shelf-slope break. This "hinge line" in Northern Egypt exerts the fundamental control on reservoir distribution in Tertiary age strata. In Late Eocene time, Northern Egypt was tilted toward the Mediterranean during the regional uplift associated with the opening of the Gulf of Suez and Red Sea rifts. Drainage systems shed reservoir quality sediments northward in a series of forced regressions. These regressions culminated in be-heading of the youngest deltas by subaerial erosion during the sea level low stand associated with the Messinian salinity crisis. Early Pliocene transgressions deposited a thick sealing interval over the low-stand Messinian valley networks.

2. LOCATION OF THE STUDY AREA

The study area lies between latitudes $31^{\circ} 3'$ & $31^{\circ} 9'$ N and longitudes $31^{\circ} 19'$ & $31^{\circ} 22'$ E. It is located in the western part of South Batra Field and lies in the central part of El Mansoura Concession northern of El Mansoura City (Figure-1).

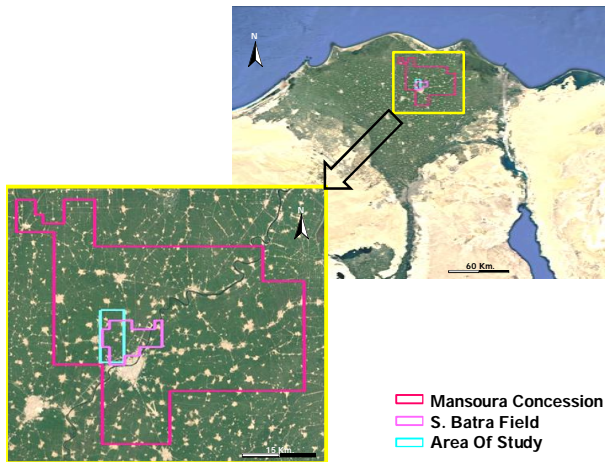


Figure 1: Geographical Location Map of the South Batra Field.

The area of study were drilled by 7 wells (Figure-2), these wells are (from south to north respectively) South batra-22, South batra-17, South batra-18, South batra-15A, Mansouriya-1, South batra-8 and Dimayrah-1. All these wells are classified as gas produced wells; except South Batra-22 is classified as dry well.

In this study, only 4 well data are available. These well data related to South Batra-8, South Batra-15A, South Batra-17 and Mansouriya-1 wells.

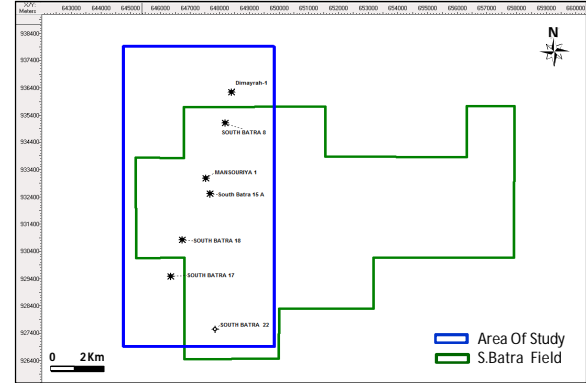


Figure 2: Location Map of the Area of Study Wells.

3. DATA AND METHODOLOGY

The present work is based on the available Pre-stack and 3D Post-stack seismic data, well logging data and subsurface borehole geological cross sections.

All types of logs such as (GR, Sonic, Density, Resistivity, Check shot) will be used. But the most important logs to perform the inversion model are sonic and density.

In this study the applied Sonic log is P-wave only while the S-wave had been calculated by using **Castagna's Equation** :

$$V_s = a * V_p + b$$

Where: $a = 0.8619$ and $b = -1172$

The S-wave is important to calculate Poisson's ratio which is equal V_p/V_s .

The 3D Post-stack seismic data were used in the seismic interpretation, the construction of a 3D structural model of the interpreted faults, horizons and to apply the Post-stack seismic inversion. While the Pre-stack seismic data were used to understand and apply the AVO analysis.

The 3D Post-stack seismic interpretation has been done on 2d/3d Pak software which is one module of Kingdom (SMT) software package. While the **AVO Analysis** and the seismic inversion has been done by using the Hampson Russell Software (HRS-9/R2) version.

As mentioned before, only 4 wells data are available. These well data are related to South Batra-8, South Batra-15A, South Batra-17 and Mansouriya-1 wells.

4. STRATIGRAPHIC SEQUENCE OF SOUTH BATRA FIELD

The stratigraphic sequence of South Batra Field comprises the following Formations from bottom to top, Sidi Salim Formation (Langhian to Tortonian), Qawasim Formation (Early Messinian), Abu Madi Formation (Late Messinian), Kafr El Sheikh Formation (Pliocene), El Wastani Formation (Late Pliocene-Pleistocene), Mit Ghamr Formation (Pleistocene/Recent) (Figure 3).

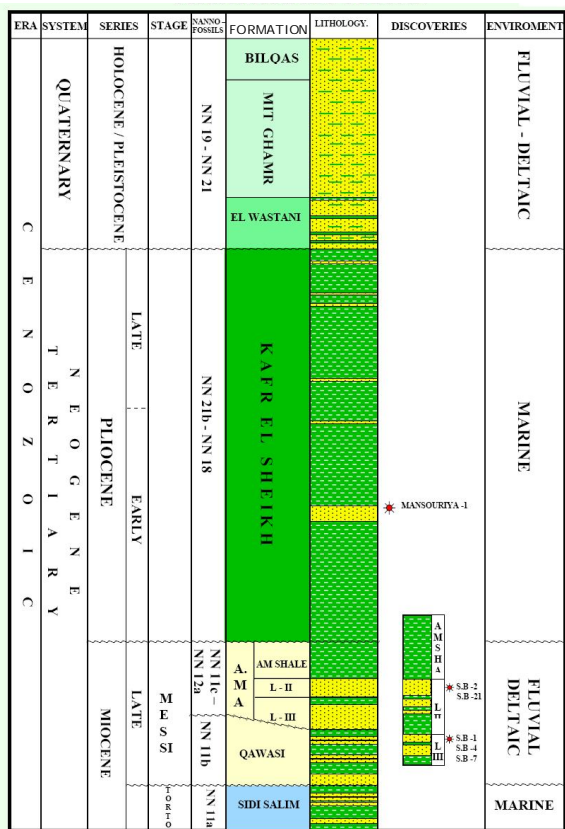


Figure 3: Generalized lithostratigraphic column of South Batra Field (Area of Study)

From the arbitrary line A-A' passing through The wells in the area of study, the regional horizons in the studied area are (Figure 4):

Top Wastani Formation, Top Kafr EL Sheikh Formation, Top Abu Madi Formation, Top Abu Madi Level II, Top Abu Madi Level III, Top Qawasim Formation and Top Sidi Salim Formation.

This study will focus only on the pay zone located in intra Kafr El-Sheik Formation (Pliocene age).

The Pliocene of the Nile Delta unconformably overlies the Messinian section below it. The Pliocene was marked by a major marine transgression which completely overstepped the Messinian incised canyons.

This resulted in the Kafr El-Sheikh marine shales being deposited at the base of the Pliocene (providing an excellent topseal for the underlying Messinian reservoirs) followed by the progradation and deposition of a thick wedge of Kafr El-Sheikh prodelta muds (Harms et al., 1990) Channel and turbidite fan sands form the reservoir units of this section while organic rich shales provide a biogenic gas source for the Kafr El-Sheikh play. The Kafr El-Sheikh is a proven gas play in the onshore and offshore Nile Delta.

A large well database is available for the Kafr El-Sheikh play, including wireline and image logs and core data.

The Kafr El-Sheikh Formation is dominated by hemipelagic shales with minor slope channel and basin floor fans. Average reservoir porosities range from 15-33% with net pay thicknesses ranging from 10-50ft.

The Kafr El-Sheikh is a shale dominated section with hundreds of feet of shale encountered in drilled wells.

Intra formational Kafr El-Sheikh shale forms the seal for the Kafr El-Sheikh play. As such seal risk for the Kafr El-Sheikh is seen as low risk throughout the Kafr El-Sheikh of El-Mansoura concession.

Hydrocarbons for the Kafr El-Sheikh play are sourced from organic-rich shale units from within the Kafr El-Sheikh. These hydrocarbons are generated by biogenic processes and as such the gas encountered in the Kafr El-Sheikh is methane rich dry gas.

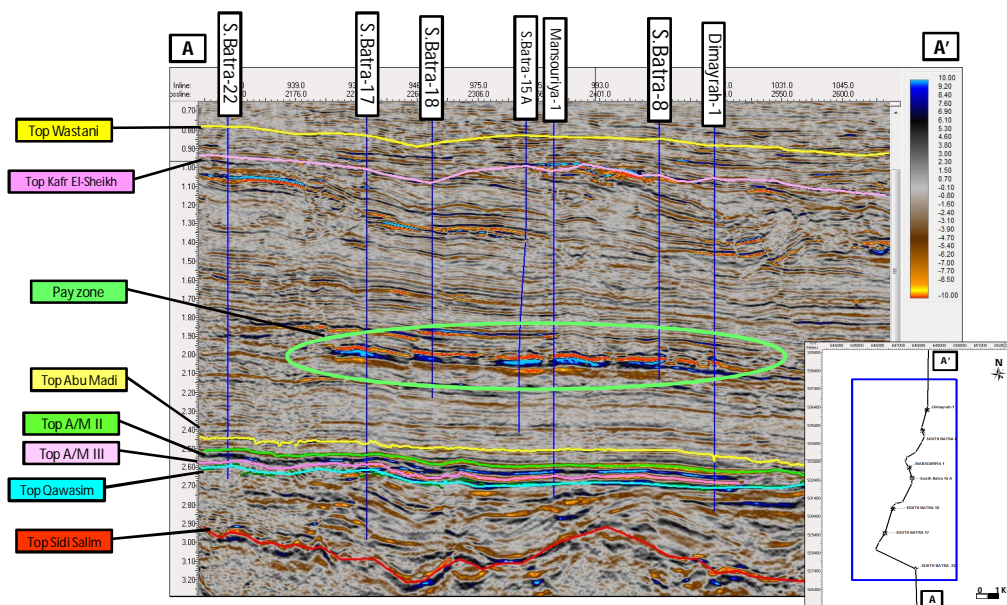


Figure 4: Arbitrary Seismic line (A-A') showing the TWT interpreted horizons.

The petroleum system of the Kafr El-Sheikh is poorly understood and discrete source beds within this formation have not been mapped. Migration pathways are also poorly understood and it is believed that Kafr El-Sheikh reservoirs are sourced directly from the surrounding Kafr El-Sheikh shales.

All mapped traps within the Kafr El-Sheikh have a major stratigraphic component present, often in the form of shelf/slope turbidite channels and basin floor fans which are encased in Kafr El-Sheikh shales.

Stratigraphic trap identification within the Kafr El-Sheikh is driven by identifying DHI's on 3D seismic as outlined in the reservoir section of this play analysis.

It is believed that biogenically produced gas migrates into Kafr El-Sheikh sand bodies directly from the encasing shales.

All the petroleum systems for the Kafr El-Sheikh; reservoir, source, seal, trap were created during the Pliocene. It is thought that gas generation and expulsion has occurred since deposition to present.

Exploration of the Kafr El-Sheikh Formation in El Mansoura concession is driven by 3D seismic coverage and interpretation. The most prospective areas for the Kafr El-Sheikh are within the submarine channel systems. Beyond these channels a moderate to low risk to prospectivity is proposed.

This correlation show the gross reservoir thickness for S.Batra-17, S.Batra-15A, Mansouria-1 and S.Batra-8 wells are 117, 99, 58 and 133ft.ss respectively.

While the net reservoir thickness for S.Batra-17, S.Batra-15A, Mansouria-1 and S.Batra-8 wells are 64, 18, 13 and 35 ft.ss respectively.

The average porosity for S.Batra-17, S.Batra-15A, Mansouria-1 and S.Batra-8 wells are 25%, 29%, 29% and 30% respectively.

While the average water saturation (Sw) for S.Batra-17, S.Batra-15A, Mansouria-1 and S.Batra-8 wells are 40%, 30%, 50% and 27% respectively.

The high reservoir thicknesses for S.Batra-17, S.Batra-15A and S.Batra-8 wells due to these wells are located in the central part of the channel sand. While the low reservoir thickness for Mansouria-1 well is due to this well is located in the levee of the channel.

The Kafr El-Sheikh sandstones for these wells are described as loose, colorless, light grey, off white, transparent to translucent, fine to very fine grained, grading to siltstone size, subrounded to subangular, moderately sorted, with argillaceous and calcareous cement and glauconitic in parts.

The sand thicknesses and the different facies for these wells are impacted on the amplitude and the

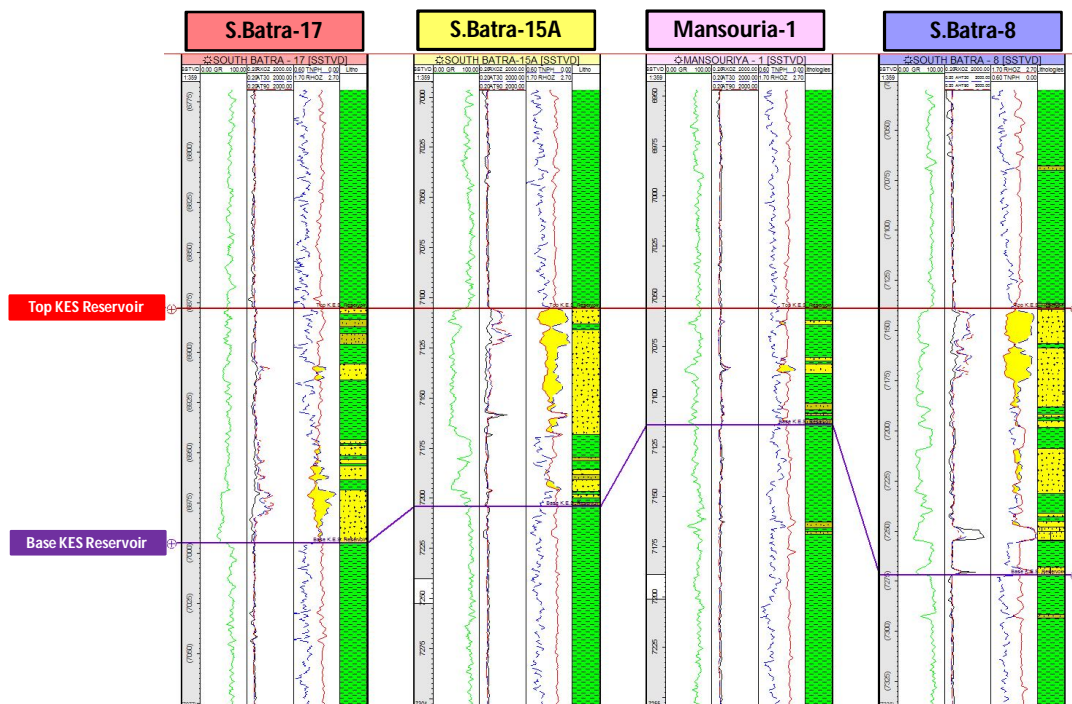


Figure 5: Well correlation for S.Batra-17, S.Batra-15A, Mansouria-1 and S.Batra-8 wells.

Represent stratigraphic correlation profile flattened on top reservoir using the information inferred from available logs, especially Sonic and composite logs for S.Batra-17, S.Batra-15A, Mansouria-1 and S.Batra-8 wells (Figure 5).

different attributes map as will shown.

5. STRUCTURE SETTING OF SOUTH BATRA FIELD

The depth structure contour map is made by using the Time-Depth relation of the wells to converting the seismic data from time domain to depth domain (Figure-6)

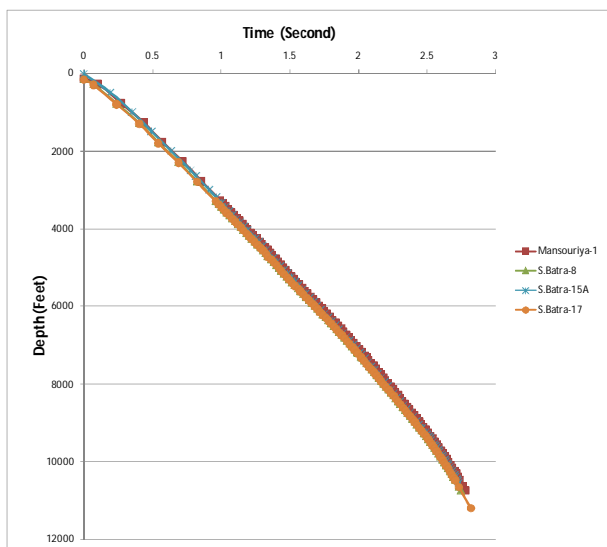


Figure 6: Time-Depth relation for S.Batra-8, S.Batra-15A, S.Batra-17 & Mansouriya-1 wells

The depth structure contour map of intra Kafr El Sheikh Sand shows the structural dip increases toward the north (Figure 7).

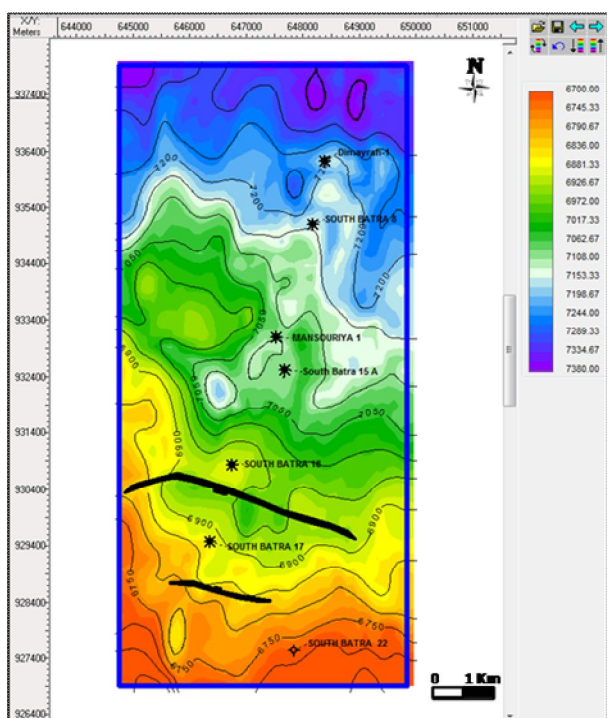


Figure 7: Depth structure contour map for intra Kafr El-Sheikh sand (C.I:50 ft).

The depth structure contour map of intra Kafr El Sheikh Sand illustrates that, the depth ranges from 6650 ft to 7300 ft and the depths increase toward the northern direction. The big thickness of Kafr El Sheikh Formation is working as a good sealing for the underlying reservoir as a cap rock.

6. RESULTS AND DISCUSSIONS

Amplitude is often found to correlate strongly with porosity and liquid saturation (oil/water vs. gas) because those reservoir properties have a strong effect on both velocity and density, and seismic reflections are generated at boundaries where the acoustic impedance (the product of velocity and density) changes. The “bright-spot” identification of hydrocarbons as demonstrated in (Figure 8).

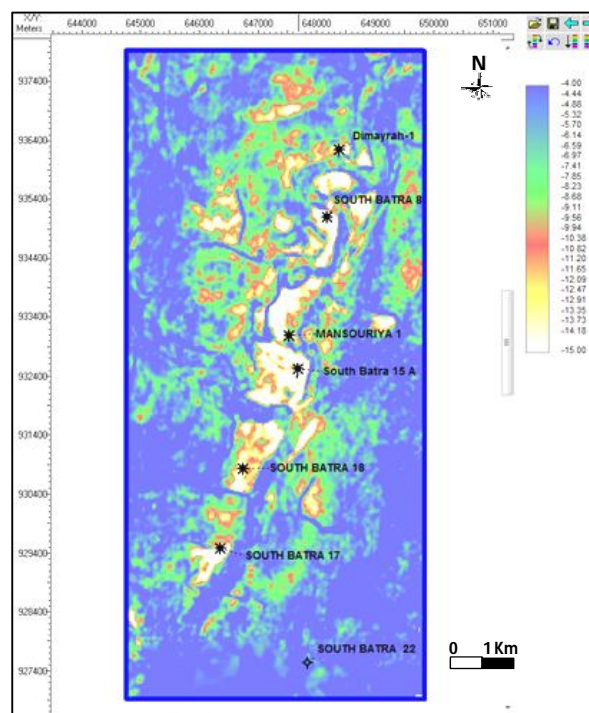


Figure-8 AVO Stack (Amplitude) map.

The amplitude map of Kafr El-Sheikh sand shows the highest negative true amplitude anomalies that tested by S.Batra-17, S.Batra-8, S.Batra-18, S.Batra-15A, Mansouria-1 and Dimairah-1 gas discovery wells, while the dimming amplitude areas were tested by S.Batra-22 dry well.

6.1. AVO Classes:

Fundamental to the use of AVO plot in interpretation is the characterization of different types of responses, depending on lithology and fluid type (Hampson et al., 2004) Shale/ Sand AVO responses are classified into four types (I, II, III & IV) depending on the impedance contrast between the shale and the sand (Figure 9). Type I responses are characterized by a positive contrast in impedance (i.e. the sand impedance is larger than the shale impedance), together with a decreasing amplitude with angle. Class II responses have small normal incidence amplitudes (positive or negative), but the AVO effect leads to high negative amplitudes at far offsets.

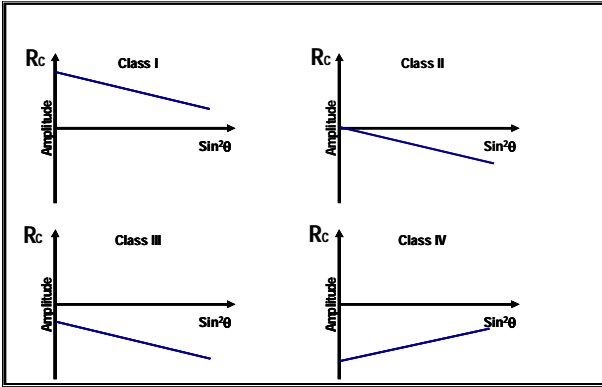


Figure 9: AVO Classes diagrams.

Some expertise in the AVO have suggested that, the small positive Class II responses should be termed Class IIp, owing to the phase reversal that is inherent in this response, and that the term Class II should apply to the small negative impedance contrast response. Class III responses have large negative impedance contrasts and the negative gradient leads to increasing amplitude with angle.

A further type of top sand response is Class IV,

these responses occur where large negative amplitude decreases slightly with offset and are characteristic of situations, where a very fast formation (such as limestone or anhydrite) lies above a gas sand or in very shallow sections, where the poisson ratio of the sands is slightly higher than the shale.

From the CDP gather of S.Batra-17 well, it's clear that the negative amplitude is gradually increase with offset, which mean that class III is present in this field (Figure 10).

From the AVO angles attributes, the maps indicate a gradual increase of the AVO amplitude anomaly from 0-10 (Near) to 10-20 (Med) then 20-30 (Far) degrees (positive AVO response), which is a good indicator for the presence of gas-bearing sand encountered by the successful wells (Figure 11).

6.2. AVO Cross Plot:

It was realized that, the cross plot of intercept and gradient provided a tool for analyzing the AVO responses and determining the appropriate use of intercept and gradient to highlight anomalies (Castgna, 1997) (Figure 12).

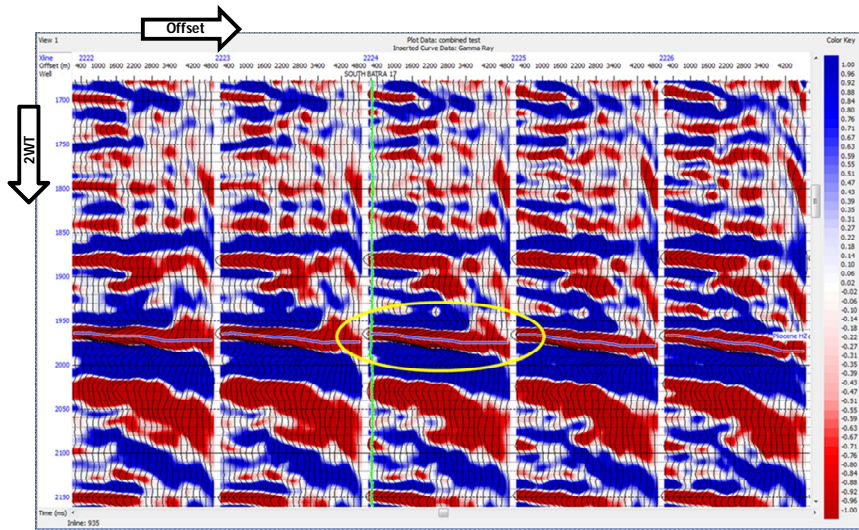


Figure 10: CDP Gather of S.Batra-17 well.

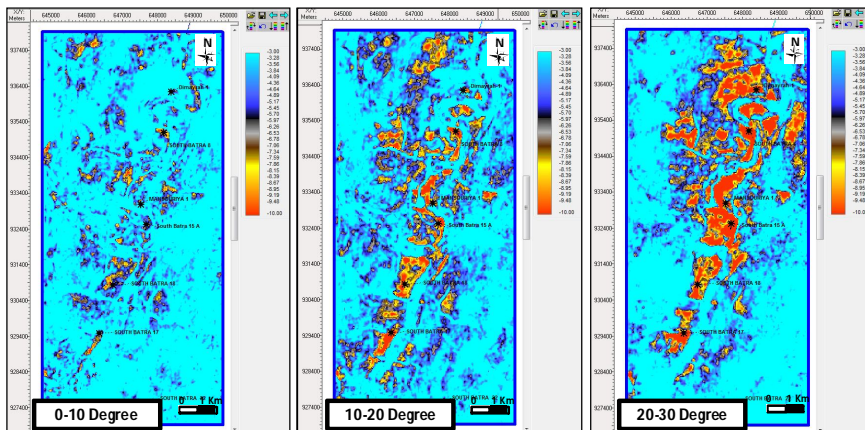


Figure 11: AVO angles (0-10),(10-20) & (20-30) degree maps.

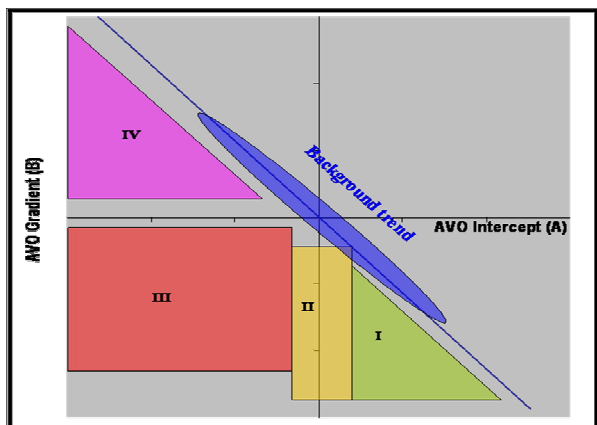


Figure 12: Cross Plot of Intercept Vs Gradient.

The AVO classes fall in particular parts of the cross plot and anomalies can be discriminated either on the basis of zones or as a result of linear combinations of the intercept and gradient (Castagna, 1998).

Intercept and gradient pairs move further away from the background trend with decreasing fluid density, so that gas sands will be the most well separated (Figure 13). The degree of shift will be controlled by the stiffness of the rock.

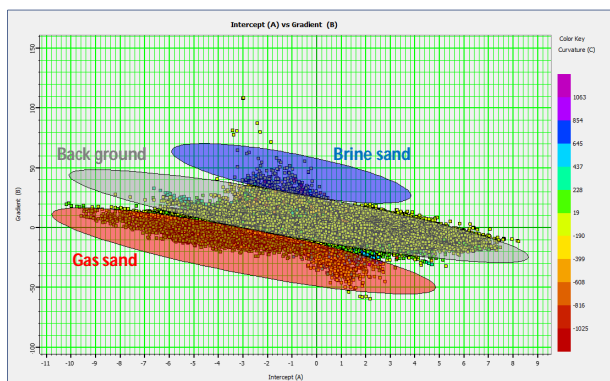


Figure 13: Cross Plot for Intercept Vs Gradient over the area of study in S.Batra Field.

From the cross plot, it's clear that class III is present in the area of study in S.Batra field. The AVO interpretation using this technique was done in this project by: (1) Background trend around the origin was defined (gray color). (2) Points, which lie outside this trend, were highlighted (red indicates gas sand zone and grey indicates brine sand zone). (3) These anomalies are dropped to the seismic and Calibrated with the well result (Figure 14).

6.3. Intercept and Gradient:

In Hampson Russell software, the calculation of intercept and gradient volumes from an input pre-stack dataset is simple. The only required information is the velocity data, in which the velocity data of S.Batra-17 well is used as velocity control.

Figure 15 illustrates the AVO response derived from the intercept and gradient volumes. In these figures, the trace data shows the intercept, while the color display represents the product of the intercept and gradient, which indicates the AVO anomaly. By calibration of this AVO anomaly with both the gamma-ray log and top pay of the wells, it is found that, there is compatibility between the AVO response, the sand reservoir and the top pay of the wells.

6.4. Poisson's Ratio Change:

Another AVO attribute called scaled Poisson's ratio change, which is considered a better way to show the AVO anomaly. Poisson's ratio is the ratio of deformation of a certain rock in different directions". Figure -16 shows this attribute, in which the trace data shows the intercept, while the color data shows the scaled Poisson's ratio change. It is found that, there is compatibility between the AVO response, the sand reservoir and the top pay of S.Batra-17, S.Batra-15A, S.Batra-8 and Mansouria-1 wells.

6.5. Post-stack Seismic Inversion:

The inverted model means to create absolute acoustic impedance from post-stack seismic data. In a seismic inversion the original reflectivity data, as typically recorded routinely, is converted from an interface property (i.e. a reflection) to a rock property known as impedance, which itself is the multiplication of sonic velocity and bulk density. In a conventional seismic reflectivity section the strong amplitudes are associated with the boundaries between geological formations, such as the top reservoir. This type of data is most suited to structural interpretation. In an inverted dataset the amplitudes are now describing the internal rock properties, such as lithology type, porosity or the fluid type in the rocks (brine or hydrocarbons). Inverted data is ideal for stratigraphic interpretation and reservoir characterization. Seismic inversion is undertaken to complement conventional deconvolution processing (Figure 17).

The acoustic impedance applied by multiplying density and sonic logs, the low acoustic impedance refer to high porosity area, while the high acoustic impedance refers to low porosity area. Inversion of seismic amplitude generated the colored-coded panel, with low acoustic impedance in green color, and high acoustic impedance in purple color.

The arbitrary line A-A' passing through the wells (Figure 18) in the inverted cube display a good correlation between the reservoir location and the low acoustic impedance areas.

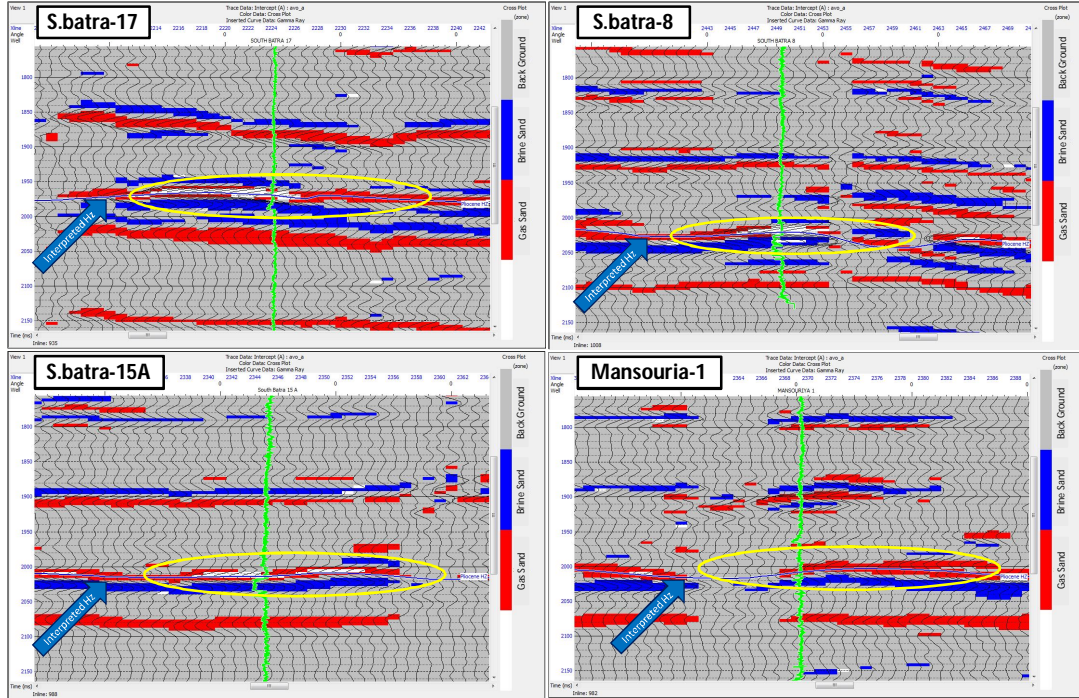


Figure 14: showing the gas sand, brine sand and the back ground trend for S.Batra-17, S.Batra-8, S.Batra-15A and Mansouria-1 wells.

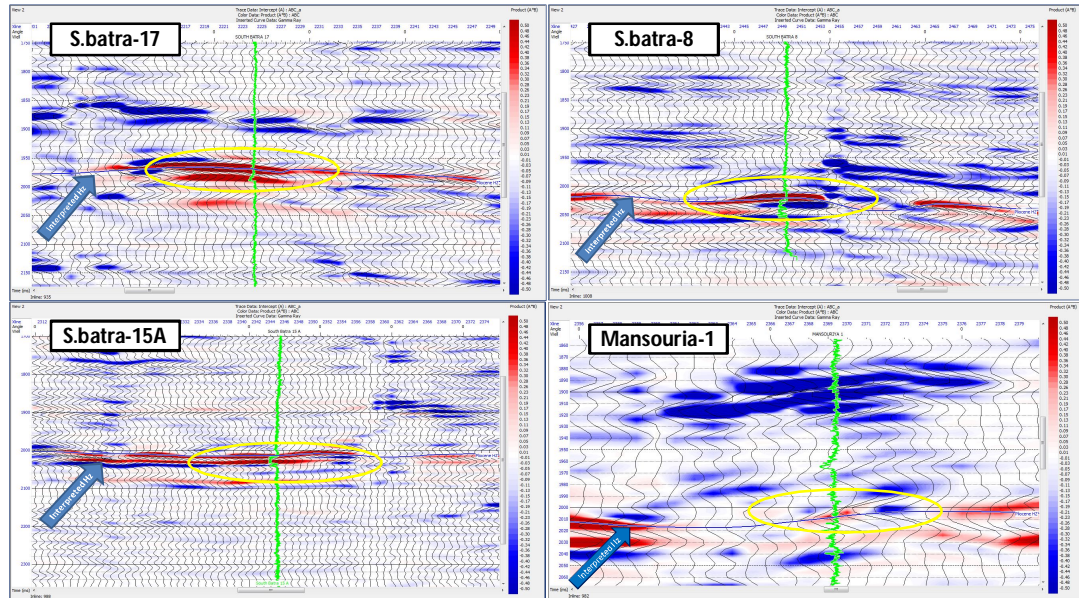


Figure 15: Product of Intercept and Gradient, as an AVO anomaly for S.Batra-17, S.Batra-8, S.Batra-15A and Mansouria-1 wells.

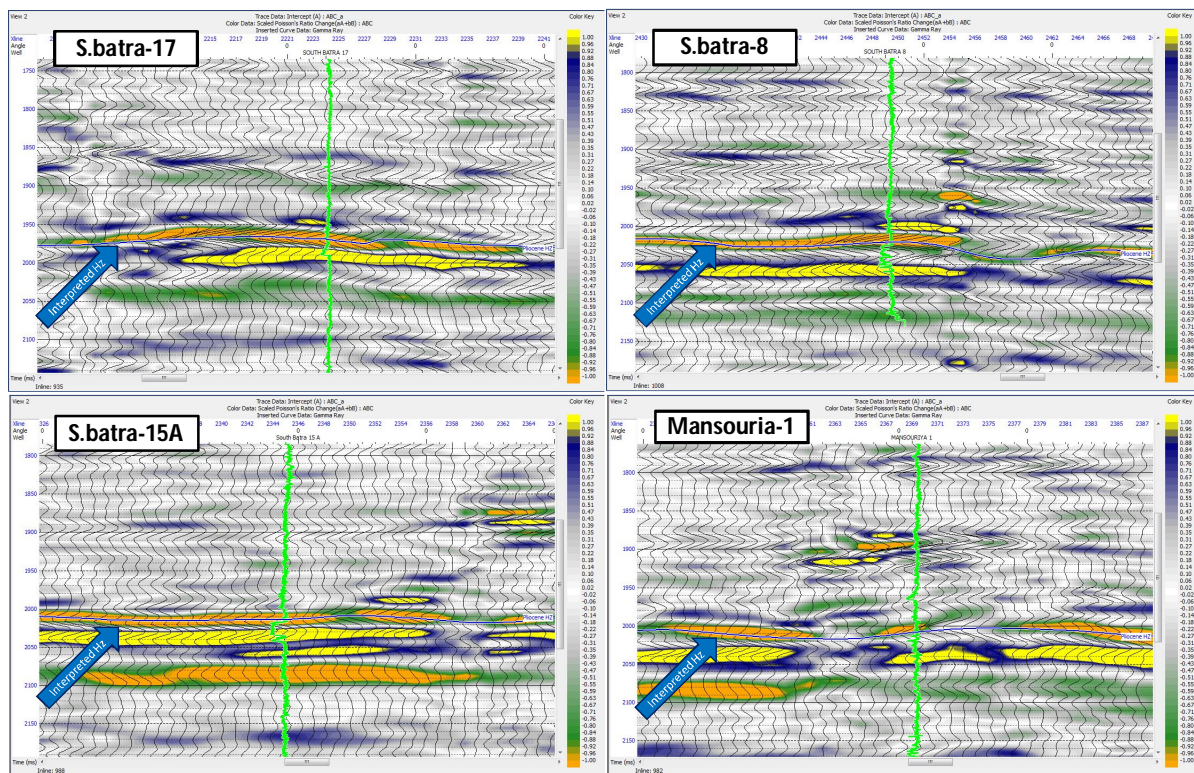
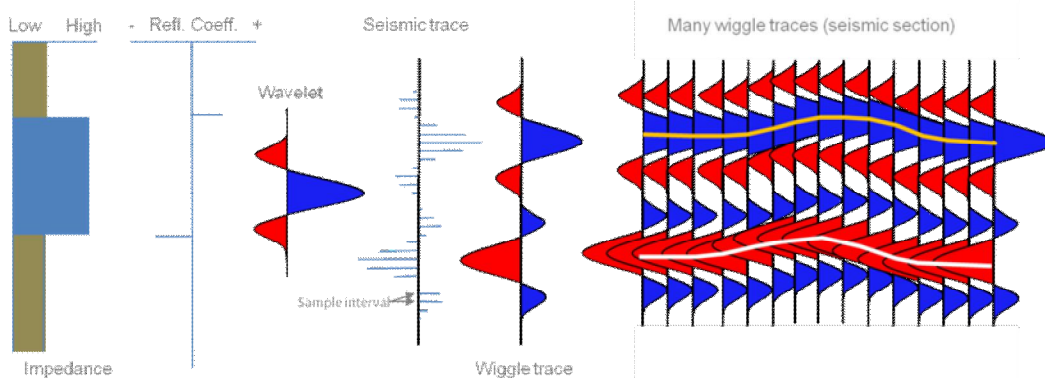


Figure 16: Change in Poisson's Ratio indicates AVO anomaly for S.Batra-17, S.Batra-8, S.Batra-15A and Mansouria-1 wells.



reflectivity * wavelet + noise = seismic

Figure 17: Showing the Convolution/Deconvolution process.

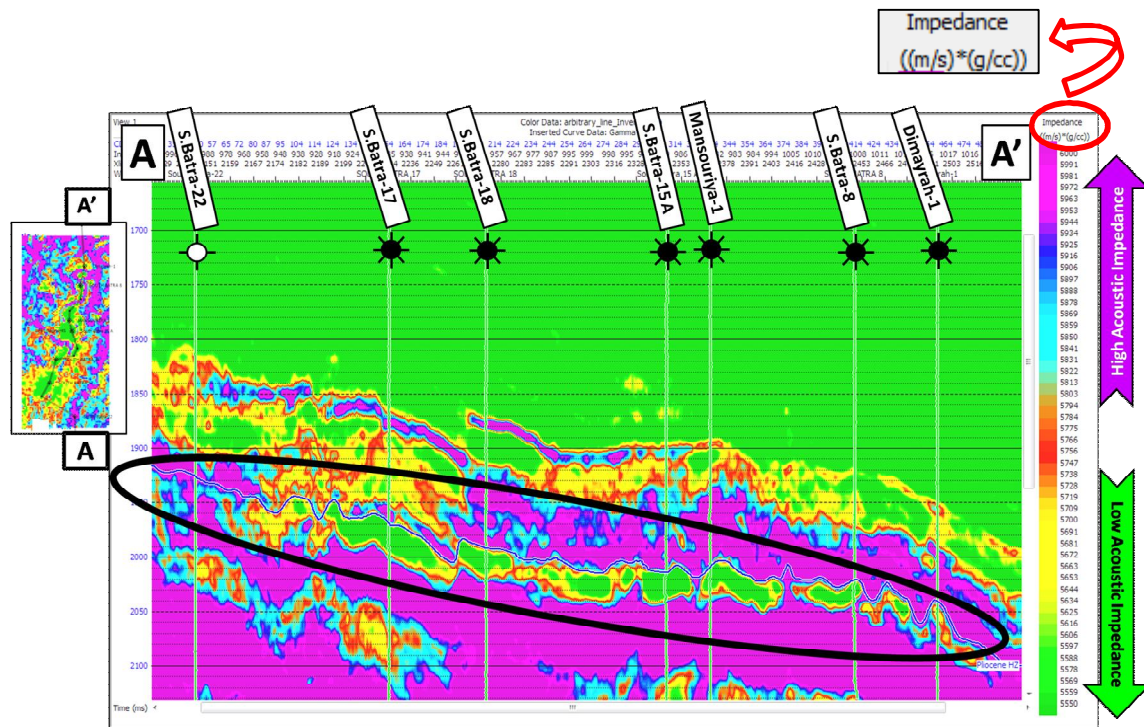


Figure 18: Arbitrary line A-A' passing through the wells in the inverted model.

7. SUMMARY AND CONCLUSION

The aim of this study is determining how to use the different seismic attributes for tracing and determining the hydrocarbon accumulation in Kafr El-Sheikh formation (Pliocene Age) in South Batra field ,El-Mansoura concession, Nile Delta –Egypt.

The study area lies between latitudes $31^{\circ} 3' & 31^{\circ} 9' N$ and longitudes $31^{\circ} 19' & 31^{\circ} 22' E$. It is located in the western part of South Batra Field and lies in the central part of El Mansoura Concession northern of El Mansoura City.

South Batra field is producing hydrocarbon from three main reservoir levels. These levels are:

- Kafr El-Sheikh formation (Pliocene Age).
- Abu Madi level II (Messinian Age).
- Abu Madi level III (Messinian Age).

This study is focusing only on the pay zone located in intra Kafr El-Sheik Formation (Pliocene age).

Amplitude is often found to correlate strongly with porosity and liquid saturation (oil/water vs. gas) because those reservoir properties have a strong effect on both velocity and density, and seismic reflections are generated at boundaries where the acoustic impedance (the product of velocity and density) changes.

The presence of gas in the sand reservoir led to increase in the amplitude as the offset increase. This is called the AVO response.

Using the pre-stack seismic data to understand the AVO, an AVO anomaly application is most commonly

expressed as increasing (rising) AVO in a sedimentary section, often where the hydrocarbon reservoir is "softer" (lower acoustic impedance) than the surrounding shales. The most important application of AVO is the detection of hydrocarbon reservoirs.

From the AVO analysis using the Hampson Russell software and by using the wells data, it is clear that South Batra field is a class III AVO (Increase of negative amplitude with offset).

Using the post-stack seismic inversion to delineate the hydrocarbon reservoir. Inversion replaces the seismic signature by a blocky response, corresponding to acoustic and/or elastic impedance layering. It facilitates the interpretation of meaningful geological and petrophysical boundaries in the subsurface. The inversion is an inverting the relative acoustic impedance values from the seismic to an absolute acoustic impedance values.

The South Batra gas field in the turbidite channel H.S.T (High Stand System Tract) of Kafr El-Sheikh formation is a stratigraphic trap with AVO class III response.

REFERENCES

- Said R., (1981) The geology and evolution of the River Nile: Springer, New York, N.Y., 151 p.
- Niazi M, Dahi M., (2010). UN Explored Giant Sandstone Features in Ultra – deep water, West Mediterranean, Egypt, E.G.P.C, Egypt.

Harms, J.C., and J.L. Wary, (1990). Nile Delta, in R. said, ed., The geology of Egypt: Rotterdam, Netherlands, A.A. Balkema Publishers, P.734

Hampson, D., Russell, B. and Cardamone, M., (2004). Uncertainty in AVO-How can we measure it? Recorder, 29, no.3, 5-11.

Castagna, J.P., Swan, H.W. (1997), principles of AVO crossplotting, The Leading Edge, 16, no. 04, 337-342.

Castagna, J.P., Swan, H.W. and Foster, D.J., (1998). Frame work for AVO gradient and intercept interpretation, Geophysics, 63, 948-956.

Internal Un-Published References:

- **El Mansoura internal report, (2005).** Final well report for South Batra-17 well.
- **El Mansoura internal report, (2005).** Final well report for South Batra-15A well.
- **El Mansoura internal report, (2005).** Final well report for South Batra-8 well.
- **El Mansoura internal report, (2003).** Final well report for Mansouria-1 well.
- **El Mansoura Regional Geology & Geophysics Report, (2010).**